

Supplemental Information

The balance between paraelectricity and ferroelectricity in non-chiral smectic homologs

Dorota Węłowska, Michał Czerwiński, Robert Dzieńisiewicz, Paweł Perkowski, Jadwiga Szydłowska, Damian Pocięcha, Mateusz Mrukiewicz*

Dorota Węłowska, Michał Czerwiński, Robert Dzieńisiewicz
Institute of Chemistry, Military University of Technology, Kaliskiego 2, 00-908 Warsaw, Poland

Paweł Perkowski, Mateusz Mrukiewicz
Institute of Applied Physics, Military University of Technology, Kaliskiego 2, 00-908 Warsaw, Poland

Damian Pocięcha, Jadwiga Szydłowska
Faculty of Chemistry, University of Warsaw, Żwirki i Wigury 101, 02-089 Warsaw, Poland

Corresponding author: mateusz.mrukiewicz@wat.edu.pl

Contents:

1. Experimental methods
2. Supplementary results
3. Chemical synthesis and characterization
4. Supplemental references

1. Experimental methods

Differential scanning calorimetry

Differential scanning calorimetry (DSC) measurements were carried out using a Netzsch DSC 204 F1 Phoenix calorimeter, which was calibrated with indium, zinc, and water standards. The heating and cooling processes were performed at a rate of 2.0 K/min, and the samples were maintained in the aluminum crucibles under a nitrogen atmosphere with a gas flow rate of 20.0 ml/min. The transition temperatures and corresponding enthalpy change values were determined from the heating and cooling curves.

Polarizing optical microscopy

Optical investigations were performed with an OLYMPUS BX51 polarized optical microscope equipped with a Linkam TMS93 temperature controller and a THMSE 600 heating stage. The samples were placed between untreated glass plates to observe their "natural" textures.

Molecular modeling

The dipole moment values for the optimized molecular geometry were computed using the GAUSSIAN 09 molecular simulation software.^[1] Structural optimization and other related calculations were performed using the B3LYP hybrid functional in conjunction with the 6-311G+(d,p) basis set, as previously described in our earlier work.^[2] A frequency analysis was conducted to ensure that the obtained conformation represented a true energy minimum.

X-ray diffraction

X-ray diffraction (XRD) studies in broad diffraction angle range were performed with a Bruker GADDS system. The system is equipped with a microfocus type X-ray tube with Cu anode and Vantec 2000 area detector. For small angle XRD experiments a Bruker Nanostar system was used with a microfocus X-ray tube with Cu anode, MRI heating stage, and Vantec 2000 area detector. In both cases samples were prepared as a droplets/thin films on a heated surface.

Second harmonic generation

In the Second Harmonic Generation (SHG) experiment, a solid-state infrared laser EKSPLA NL202 was used. Laser radiation with a wavelength of $\lambda = 1064$ nm incident perpendicularly

onto a planarly aligned cell of thickness 5 μm . To avoid material decomposition, the pulse energy was adjusted. The laser generated the 9 ns pulses at a 10 Hz repetition rate with a maximum energy of 2 mJ. At the entrance to the cell, an IR filter was installed on the setup, whereas a green filter was placed at the output of the SHG signal from the sample.

Spontaneous electric polarization

The triangle-wave technique was used to induce the repolarization current. The electric signal of frequency 1 Hz was applied by a Hewlett Packard 33120A waveform generator and gained using an FLC Electronics F20ADI voltage amplifier. The voltage drop across a 10 k Ω resistor was registered on a Hewlett Packard 54601B oscilloscope. To calculate the spontaneous polarization P_S value, the peak current was integrated in the time domain using the following formula:

$$P_S = \int \frac{I_P}{2S} dt \quad (1)$$

where S is the active electrode area, I_P is the polarization current flowing through the cell after the separation of the capacitor charging current and the ionic current. The temperature was stabilized using a Linkam TMS 93 temperature controller with a THMSE 600 heating stage. The measurements were done in 5 μm thick cell without any aligning layers.

Dielectric Spectroscopy

The complex electric permittivity ε^* was measured at low (0.1 V) signal voltage over the frequency f range from 100 Hz to 10 MHz by using a Hewlett Packard 4294A impedance analyzer. The dielectric studies were performed in 5 μm thick cells with low resistivity (10 Ω/sq) ITO electrodes. Cells without alignment polyimide layers were used. The temperature was stabilized with 0.1 $^\circ\text{C}$ accuracy using a Linkam TMS 92 temperature controller with a THMSE 600 heating stage. The calculated real ε' and imaginary ε'' parts of electric permittivity were fitted to the Cole-Cole model^[3] with the ionic contribution to determine the dielectric strength $\delta\varepsilon_i$ and characteristic relaxation frequency f_{R_i} of the i^{th} relaxation mode:

$$\varepsilon^* = \varepsilon_\infty + \sum_i \frac{\delta\varepsilon_i}{1 + \left(j\frac{f}{f_{R_i}}\right)^{1-\alpha_i}} - j\frac{\sigma}{2\pi f \varepsilon_0}, \quad (2)$$

where ϵ_0 is the electric permittivity of free space, ϵ_∞ is the high-frequency limit of permittivity, α is the distribution parameter, and σ represents conductivity due to the electrode polarization process visible in dielectric spectra at low frequencies (below 1 kHz).

2. Supplementary results

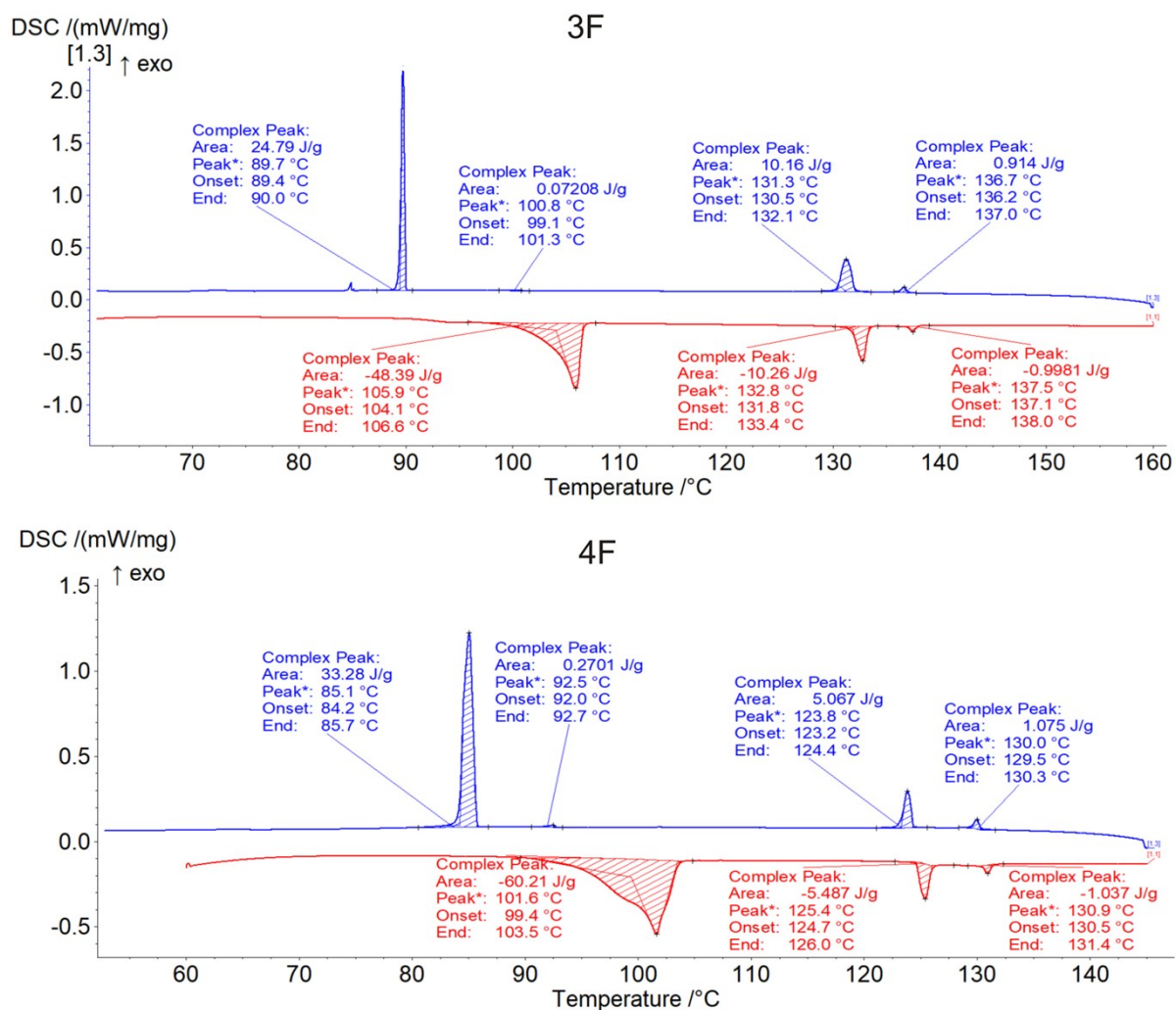


Figure S1. The DSC tracers of compounds 3F and 4F in the heating cycles (down curves) and cooling cycles (upper curves).

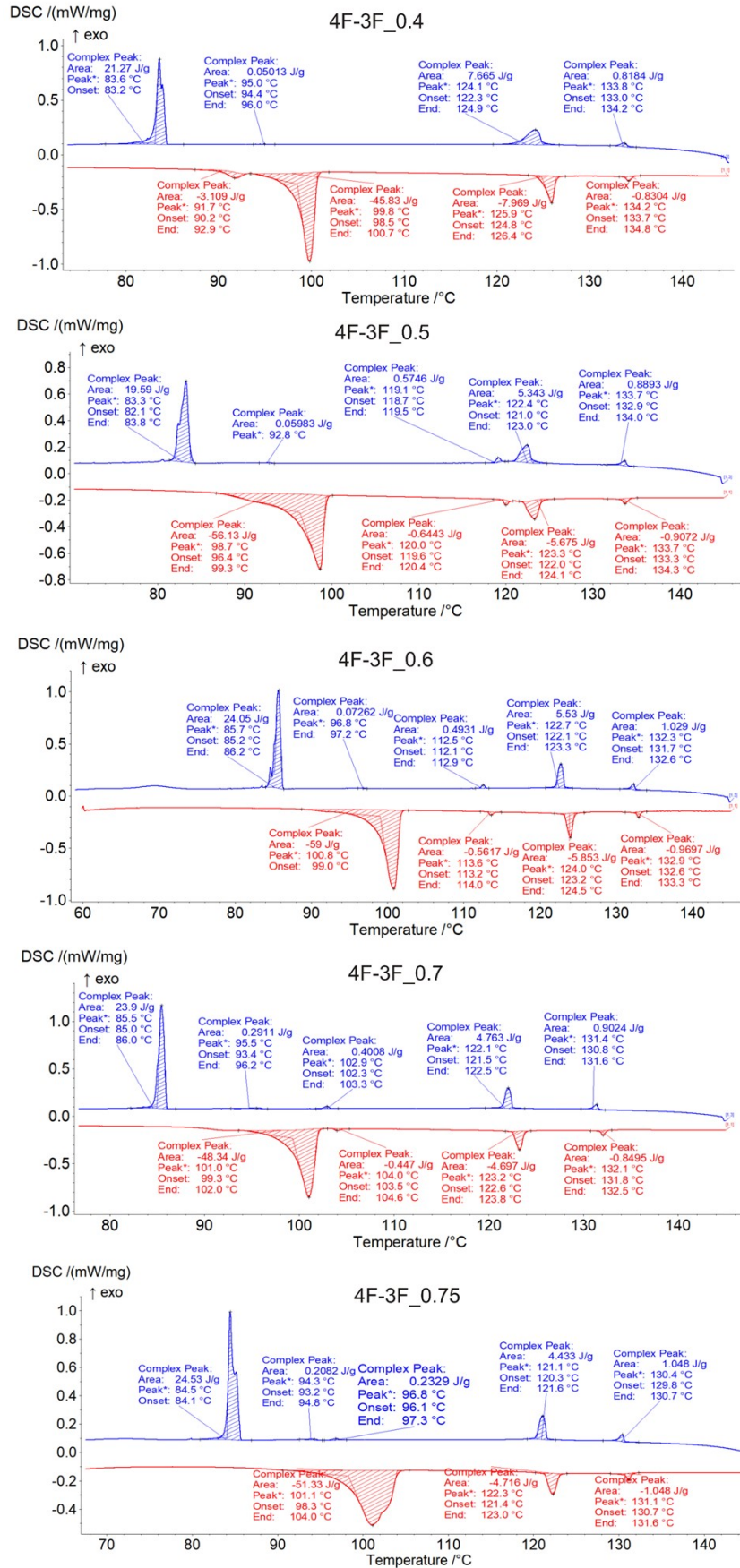


Figure S2. The DSC tracers of mixtures 4F-3F in the heating cycles (down curves) and cooling cycles (upper curves).

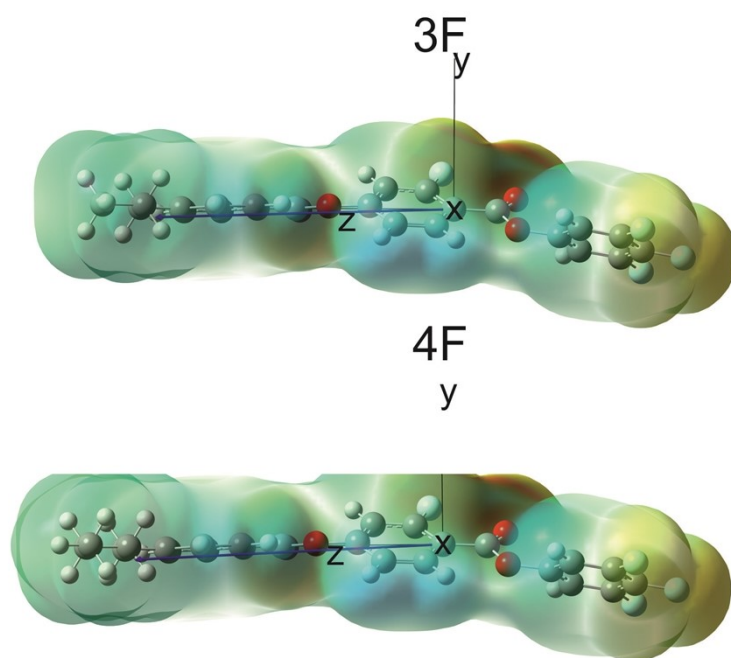


Figure S3. The optimized geometric general structure of compounds 3F and 4F aligned along the principal molecular axis with a blue arrow showing the direction of the molecular dipole moment; whereas x is the axis in the plane of the phenyl rings, y - is the axis perpendicular to the plane of the phenyl rings and z -the axis along to the principal molecular axis.

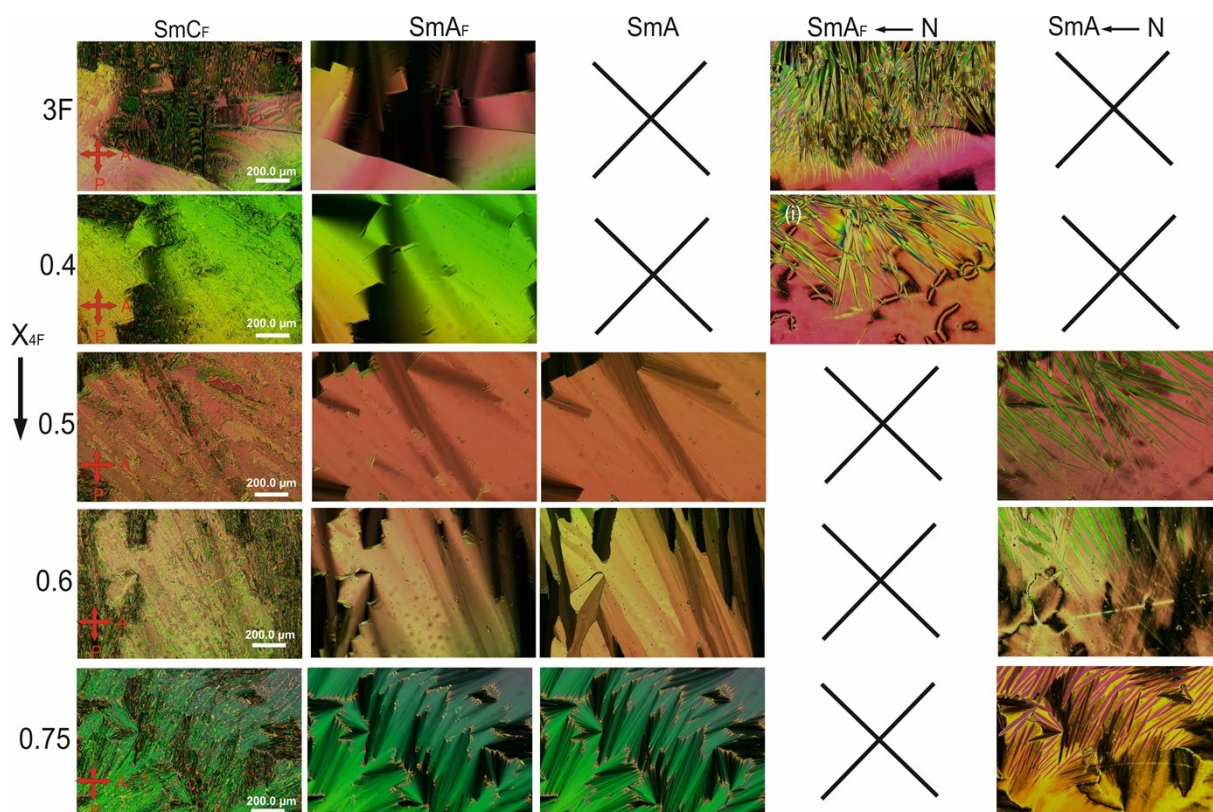


Figure S4. The POM texture evolution of 3F compound and mixtures 4F-3F system during the cooling process under crossed polarizers for LC filled between untreated glass plates.

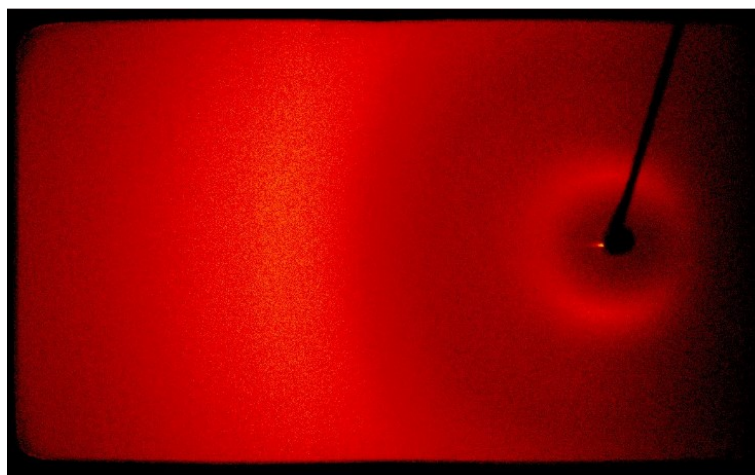


Figure S5. XRD diffraction pattern in the nematic phase (135°C) of 3F.

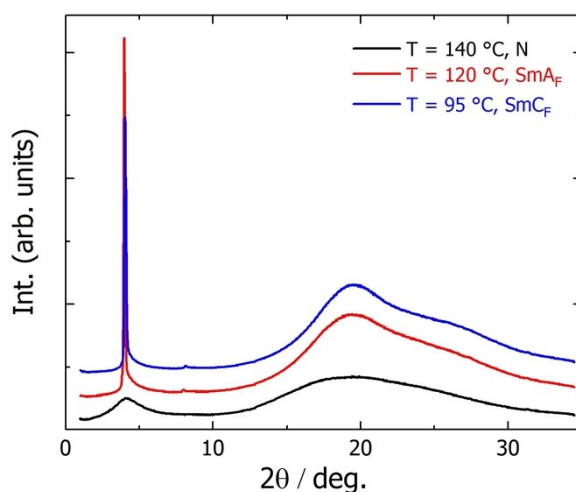


Figure S6. Broad-angle XRD diffractograms recorded in LC phases of compound 3F.

3. Chemical synthesis and characterization

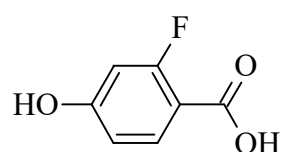
Preparative procedures

All chemicals and solvents were used as purchased (J.T. Baker, TM; POCH S.A., Sigma-Aldrich, Avantor Performance Materials Poland S.A, and Merck) and used as received. The purity of intermediates and the main compounds were determined by thin layer chromatography (TLC; with a DCM as an eluent and SiO₂ as a stationary phase and visualized with 254 or 365 nm UV light), GC-MS(EI) (Agilent 6890N, Santa Clara, CA, USA), and HPLC-PDA-MS (API-ESI dual source) (Shimadzu LCMS 2010 EV) chromatography systems using Kinetex EVO C18 column with a particle size of 2.6 μm,

dimensions of 150×4.6 mm and pore size of 100 Å (Phenomenex, USA) and a diode array detector (SPD-M20A). The mobile phases consisted of ACN/H₂O at 90/10 (v/v). The structures of the final compounds were confirmed by mass spectra registered on the HPLC chromatography system with a diode array detector (SPD-M20A) and mass detector (LCMS-85 2010EV) and by ¹H, ¹³C NMR and ¹⁹F NMR spectroscopy (Bruker, Avance III HD, 500 Hz; CDCl₃, Billerica, MA, USA).

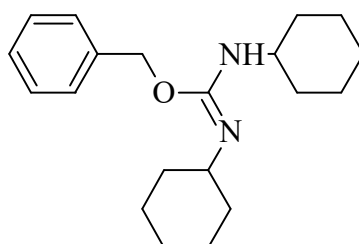
Synthetic procedures are described for an exemplary compound **3F**.

2-fluoro-4-hydroxybenzoic acid (1)



A mixture of ethyl 2-fluoro-4-hydroxy benzoate (15.0 g, 81 mmol), potassium hydroxide (18.8 ml, 334 mol) in water (25 ml) and ethanol (100 ml) was refluxed for 6 hours. When the reaction was complete (TLC), the reaction mixture was poured into 2M HCl (100 ml), stirred, and concentrated at low pressure. The crude product crystallized from water (100 ml). Yield: 10.6 g (85%); M_p=195–197°C. GC: 99.8 %; MS(EI) m/z: 156 [M+H]⁺. Chemical shifts of ¹⁹F NMR resonance was similar to the published values.^[4]

Benzyl N, N'-dicyclohexylimidocarbamate (2)

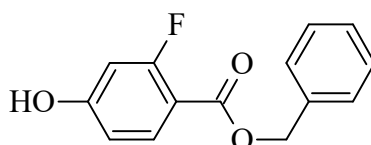


A mixture of N, N'-dicyclohexylcarbodiimide (25.2 g, 120 mmol), benzyl alcohol (13.5 g, 130 mmol), toluene (40 ml), and a bit of copper (I) chloride was stirred at room temperature for 5 days. When the reaction was complete (TLC), toluene evaporated at low pressure, hexane (250 ml) was added, and the mixture passed through an alumina pad. The filtrate was evaporated to dryness. Yield: 34.6 g (88%); B_p=130°C/0.0001 Torr.

^1H NMR (500 MHz, CDCl_3) δ /ppm: ^1H NMR: δ 1.4 (m, 12H, $-\text{CH}_2-$), 1.7 (m, 8H, $-\text{CH}_2-$), 3.0 (tt, $J=10.1, 2.6$ Hz, 1H, $-\text{CH}-$), 3.2 (tt, $J=10.1, 2.6$ Hz, 1H, $-\text{CH}-$), 5.1 (s, 2H, $-\text{CH}_2-$), 7.2 (tt, $J=7.5, 1.1$ Hz, 2H, Ar-H), 7.3 (tdd, $J=7.5, 1.4, 0.4$ Hz, 2H, Ar-H), 7.5 (m, 2H, Ar-H).

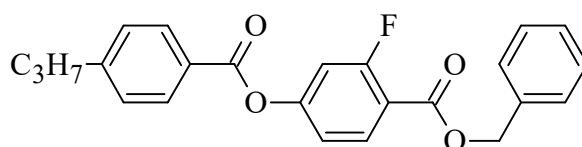
^{13}C NMR (126 MHz, CDCl_3) δ /ppm: 24.8 (s, 4C), 25.0 (s, 4C), 25.6 (s, 2C), 25.8 (s, 2C), 32.8 (s, 4C), 33.0 (s, 4C), 50.2 (s, 1C), 54.7 (s, 1C), 67.5 (s, 1C), 127.0 (s, 2C), 128.0 (s, 1C), 128.3 (s, 2C), 136.1 (s, 1C), 151.7 (s, 1C).

Benzyl 2-fluoro-4-hydroxybenzoate (3)



A mixture of 2-fluoro-4-hydroxybenzoic acid (10.6 g, 68 mmol), O-benzyl-N, N'-dicyclohexylisourea (21.4 g, 68 mmol), and dry THF (100 ml) was stirred at room temperature for 6 hours. The precipitate was filtered off, and the filtrate was concentrated at low pressure. The crude product was crystallized from ethanol (100 ml) and hexane=toluene(2:1, 100 ml). Yield: 4.5 g (27%); $M_p=90-92^\circ\text{C}$, GC: 99.8 %; MS(EI) m/z : 246 $[\text{M}+\text{H}]^+$. Chemical shifts of ^1H NMR and ^{13}C NMR resonance compound were similar to the published values.^[5]

benzyl 2-fluoro-4-[(4-propylbenzoyl)oxy]benzoate (4)



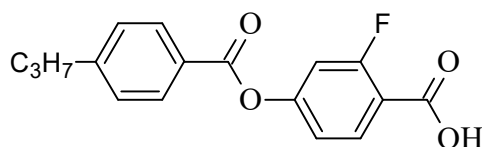
A 250 ml round-bottom flask was charged with benzyl 2-fluoro-4-hydroxybenzoate (2.3 g, 9.3 mmol), pyridine (1.5 g, 18.7 mmol), and dry dichloromethane (35 ml). The 4-propylbenzoyl chloride (1.7 g, 9.3 mmol) was dropped. The reaction mixture was stirred and refluxed until the reaction was complete (TLC). After cooling to room temperature, the reaction mixture was poured into diluted hydrochloric acid and stirred until the precipitate of pyridine hydrochloride was dissolved. Phases were separated. The water phase was extracted with dichloromethane (3 *100 ml). The combined organic fractions were washed with diluted hydrochloric acid (3*100 ml) and water (3*100 ml), dried over MgSO_4 , and concentrated in a

vacuum. The crude product was purified by column chromatography ($\text{SiO}_2/\text{CH}_2\text{Cl}_2$) obtaining colorless oil. Yield: 3.2 g (90%); GC: 98.6 %; MS(EI) m/z : 392 $[\text{M}+\text{H}]^+$

^1H NMR (500 MHz, CDCl_3) δ/ppm : 1.0 (t, $J=7.3$ Hz, 3H, $-\text{CH}_3$), 1.7 (td, $J=15.0, 7.3$ Hz, 2H, $-\text{CH}_2-$), 2.7 (m, 2H, $-\text{CH}_2-$), 5.3 (s, 2H, $-\text{CH}_2-$), 7.0 (dd, $J=7.6, 5.8$ Hz 1H, Ar-H), 7.3 (m, 5H, Ar-H), 7.4 (d, $J=8.2$ Hz, 2H, Ar-H), 7.5 (dd, $J=7.7$ Hz, 2H, Ar-H), 8.1 (s, 2H, Ar-H), 8.2 (s, 1H, Ar-H).

^{13}C NMR (126 MHz, CDCl_3) δ/ppm : 13.4 (s, 1C), 23.9 (s, 1C), 37.9 (s, 1C), 66.7 (s, 1C), 106.9 (dd, $J=10.4, 5.8$ Hz, 2C), 118.2 (s, 1C), 121.0 (s, 1C), 127.2 (s, 1C), 128.1 (s, 2C), 128.5 (s, 2C), 128.9 (2C, s), 131.4 (s, 2C), 132.8 (s, 1C), 135.0 (t, $J=15.1$ Hz, 1C), 150.9 (s, 1C), 151.4 (s, 1C), 162.5 (1C, s), 164.8 (s, 1C), 167.2 (s, 1C).

2-fluoro-4-[(4-propylbenzoyl)oxy]benzoic acid (5)

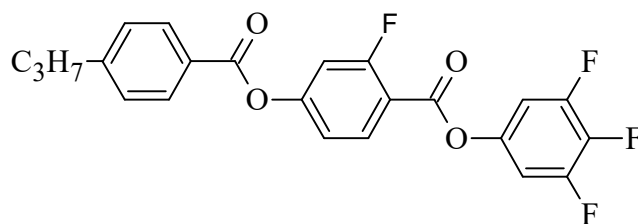


To the solution of benzyl 4-(4-propylbenzoyloxy)-3-fluorobenzoate (3.6 g, 9.2 mmol) in THF (50 ml), 10% palladium on charcoal (0.5 g) was added. The reaction mixture was flushed with hydrogen and connected to a gas burette filled with hydrogen. Stirring was turned on. While hydrogen was consumed, the temperature increased. When the reaction was completed (TLC), the reaction mixture was flushed with nitrogen, and the catalyst was filtered off and rinsed with THF (20 ml). The filtrate was evaporated, and the dry residue was crystallized from ethanol (80 ml). Yield: 1.6 g (56.7%); GC: 99.7%; MS(EI) m/z : 302 $[\text{M}+\text{H}]^+$

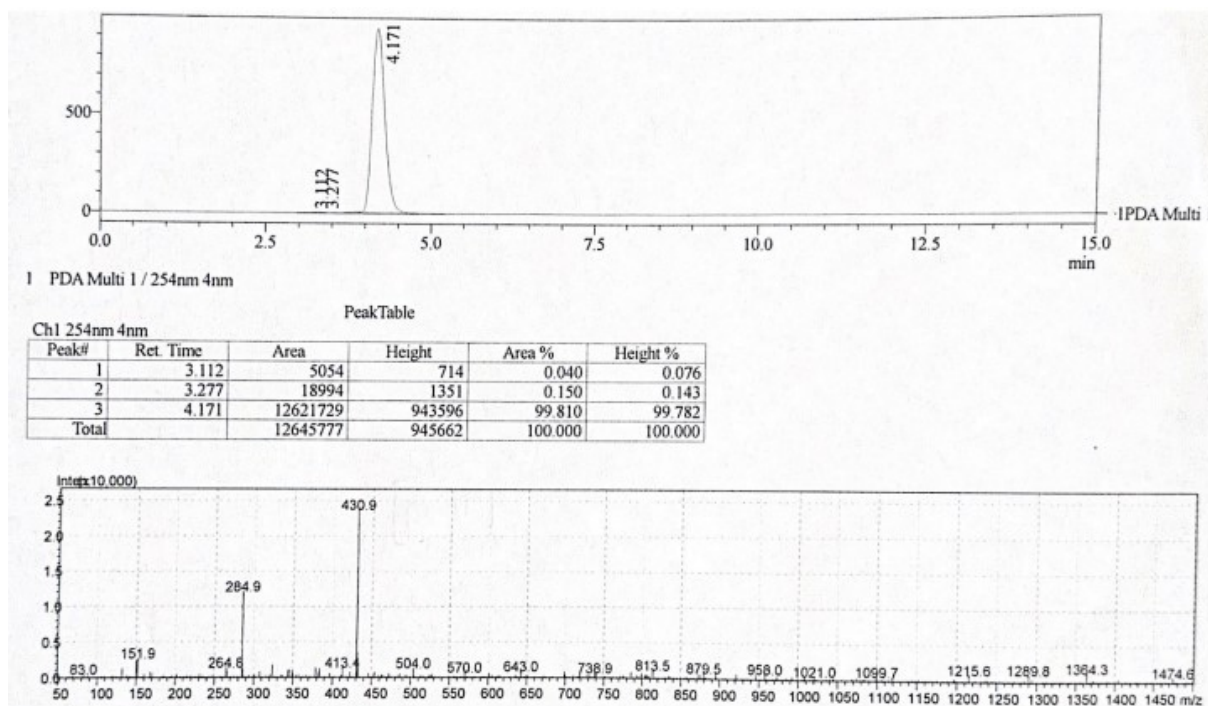
^1H NMR (500 MHz, CDCl_3) δ/ppm : 1.0 (t, $J=7.3$ Hz, 3H, $-\text{CH}_3$), 1.7 (td, $J=15.0, 7.3$ Hz, 2H, $-\text{CH}_2-$), 2.7 (m, 2H, $-\text{CH}_2-$), 7.0 (dd, $J=7.6, 5.8$ Hz 1H, Ar-H), 7.4 (d, $J=8.2$ Hz, 2H, Ar-H), 7.5 (dd, $J=7.7$ Hz, 2H, Ar-H), 8.1 (s, 2H, Ar-H), 8.2 (s, 1H, Ar-H), 12.4 (s, 1H, $-\text{O}-\text{H}$).

^{13}C NMR (126 MHz, CDCl_3) δ/ppm : δ 13.4 (s, 1C), 23.9 (s, 1C), 37.9 (s, 1C), 102.0 (dd, $J=10.0, 5.6$ Hz, 2C), 116.0 (s, 1C), 121.0 (1C, s), 128.7 (s, 2C), 129.7 (s, 2C), 131.8 (t, $J=15.4$ Hz, 1C), 149.7 (td, $J=11.2, 4.0$, 1C), 150.0 (dd, $J=10.6, 5.0$ Hz 1C), 161.9 (s, 1C), 163.4 (s, 1C), 164.0 (s, 1C).

3,4,5-trifluorophenyl 2-fluoro-4-[(4-propylbenzoyl)oxy]benzoate **3F**



To the suspension of 4-(4-propylbenzoyloxy)-2-fluoro benzoic acid (0.9 g, 2.3 mmol) in dry dichloroethane (50 ml) oxalyl chloride (0.57 g, 4.5 mmol) and one drop of N, N-dimethylformamide was added. The reaction mixture was stirred at room temperature until the evolution of gases stopped. The excess of oxalyl chloride was distilled off with dichloroethane (10 ml). After cooling to room temperature, pyridine (0.7 g, 8.9 mmol), 3,4,5-trifluorophenol (0.44 g, 3.0 mmol), and dichloromethane (10 ml) was added, and the mixture was refluxed for 6 hours. The reaction mixture was cooled to room temperature and poured into diluted hydrochloric acid (50 ml). Phases were separated. The water phase was extracted with dichloromethane (2*50 ml). The combined organic fractions were washed with diluted hydrochloric acid (3*50 ml), water (3*50 ml), and brine (50 ml), dried over MgSO₄, and concentrated at low pressure. The crude product was purified by column chromatography (SiO₂/CH₂Cl₂) and crystallized from ethanol (50 ml). Yield: 0,7 g (70%); HPLC: 99.8%; MS(EI) m/z: 431 [M-H]⁺.

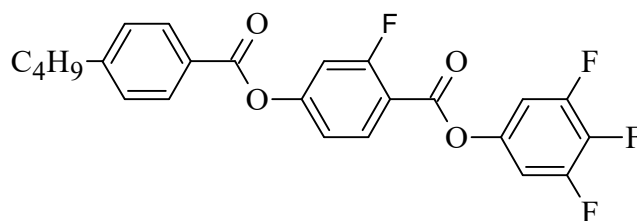


^1H NMR (500 MHz, CDCl_3) δ /ppm: 1.0 (t, $J=7.3$ Hz, 3H, $-\text{CH}_3$), 1.7 (td, $J=15.0, 7.3$ Hz, 2H, $-\text{CH}_2-$), 2.7 (m, 2H, $-\text{CH}_2-$), 7.0 (dd, $J=7.6, 5.8$ Hz 2H, Ar-H), 7.2 (m, 2H, Ar-H), 7.4 (d, $J=8.2$ Hz, 2H, Ar-H), 8.1 (s, 2H, Ar-H), 8.2 (s, 1H, Ar-H).

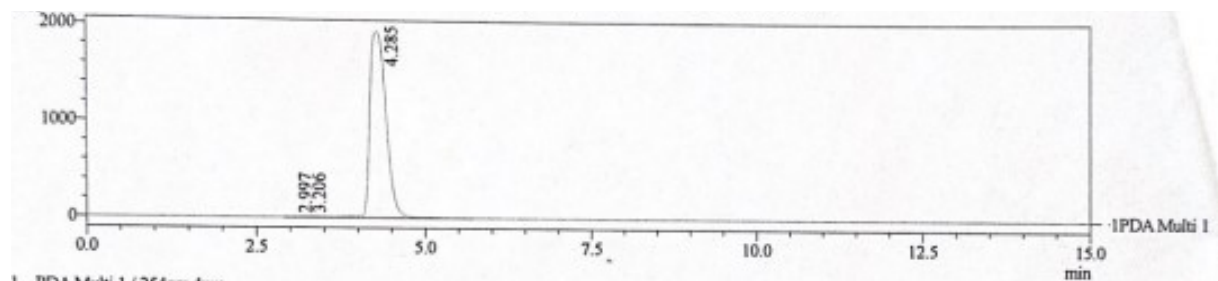
^{13}C NMR (126 MHz, CDCl_3) δ /ppm: 13.4 (s, 1C), 23.9 (s, 1C), 37.9 (s, 1C), 106.9 (dd, $J=11.2, 5.2$ Hz, 2C), 111.1 (s, 2C), 114.1 (d, $J=9.1$ Hz, 1C), 128.7 (s, 3C), 130.1 (s, 3C), 137.0 (t, $J=15.4$ Hz, 1C), 144.8 (td, $J=11.6, 4.1$ Hz, 2C), 149.7 (s, 2C), 149.8 (dd, $J=10.4, 5.0$ Hz, 1C), 161.5 (s, 1C) 163.6 (s, 1C), 163.8 (s, 1 C).

^{19}F NMR (470 MHz, CDCl_3) δ : -103.9 (t, $J=8.5$ Hz, 1F); -132.6 (dd, $J=20.7, 7.6$ Hz, 2F), -163.1 (tt, $J=20.7, 5.4$ Hz, 1F).

3,4,5-trifluorophenyl 2-fluoro-4-[(4-butylbenzoyl)oxy]benzoate 4F

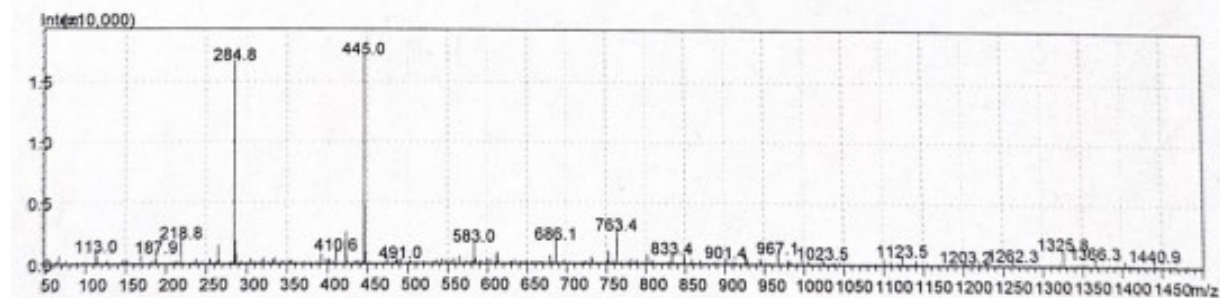


Yield: 0,6 g (59%); HPLC: 99.9%; MS(EI) m/z : 445 $[\text{M}-\text{H}]^+$.



PeakTable

Peak#	Ret. Time	Area	Height	Area %	Height %
1	2.997	4970	838	0.015	0.043
2	3.206	37788	2937	0.116	0.150
3	4.285	32452480	1948908	99.868	99.807
Total		32495237	1952682	100.000	100.000



^1H NMR (500 MHz, CDCl_3) δ /ppm: 0.9 (t, $J=7.5$ Hz, 3H, $-\text{CH}_3$), 1.4 (td, $J=7.8, 7.1$ Hz, 2H, $-\text{CH}_2-$), 1.6 (m, 2H, $-\text{CH}_2-$), 2.7 (m, 2H, $-\text{CH}_2-$), 7.0 (dd, $J=7.6, 5.8$ Hz, 2H Ar-H), 7.2 (m, 2H Ar-H), 7.3 (d, $J=8.2$ Hz, 2H Ar-H), 8.1 (d, $J=8.2$ Hz, 2H Ar-H), 8.1 (m, 1H Ar-H).

^{13}C NMR (126 MHz, CDCl_3) δ /ppm 13.9 (s, 1C), 22.3 (s, 1C), 33.2 (s, 1C), 35.8 (s, 1C), 107.2 (dd, $J=11.0, 5.4$ Hz, 2C), 111.3 (s, 2C), 114.3 (d, $J=9.1$ Hz, 1C), 128.9 (s, 3C), 130.4 (s, 3C), 137.2 (t, $J=15.4$ Hz, 1C), 145.1 (td, $J=11.4, 4.2$ Hz 2C), 150.1 (dd, $J=10.4, 5.0$ Hz, 2C), 161.3 (d, $J=4.5$ Hz, 1C) 161.8 (s, 1C) 163.9 (s, 1C) 164.0 (s, 1C).

^{19}F NMR (470 MHz, CDCl_3) δ : -103.9 (t, $J=9.9$ Hz, 1F); -132.6 (dd, $J=20.6, 7.4$ Hz, 2F), -163.1 (tt, $J=20.7, 5.1$ Hz, 1F).

4. Supplemental references

- [1] M. J. Frisch, G. W. Trucks, H. B. Schlegel, G. E. Scuseria, M. A. Robb, J. R. Cheeseman, G. Scalmani, V. Barone, G. A. Petersson, H. Nakatsuji, X. Li, M. Caricato, A. V. Marenich, J. Bloino, B. G. Janesko, R. Gomperts, B. Mennucci, H. P. Hratchian, J. V. Ortiz, A. F. Izmaylov, J. L. Sonnenberg, Williams, F. Ding, F. Lipparini, F. Egidi, J. Goings, B. Peng, A. Petrone, T. Henderson, D. Ranasinghe, V. G. Zakrzewski, J. Gao, N. Rega, G. Zheng, W. Liang, M. Hada, M. Ehara, K. Toyota, R. Fukuda, J. Hasegawa, M. Ishida, T. Nakajima, Y. Honda, O. Kitao, H. Nakai, T. Vreven, K. Throssell, J. A. Montgomery Jr., J. E. Peralta, F. Ogliaro, M. J. Bearpark, J. J. Heyd, E. N. Brothers, K. N. Kudin, V. N. Staroverov, T. A. Keith, R. Kobayashi, J. Normand, K. Raghavachari, A. P. Rendell, J. C. Burant, S. S. Iyengar, J. Tomasi, M. Cossi, J. M. Millam, M. Klene, C. Adamo, R. Cammi, J. W. Ochterski, R. L. Martin, K. Morokuma, O. Farkas, J. B. Foresman, D. J. Fox, **2016**.
- [2] D. Węglowska, M. Czerwiński, P. Kula, M. Mrukiewicz, R. Mazur, J. Herman, *Fluid Phase Equilibria* **2020**, 522, 112770.
- [3] K. S. Cole, R. H. Cole, *Journal of Chemical Physics* **1941**, 9.
- [4] W. J. H. Van Berkel, M. H. M. Eppink, W. J. Middelhoven, J. Vervoort, I. M. C. M. Rietjens, *FEMS Microbiology Letters* **1994**, 121, 207–215.
- [5] G. J. Strachan, E. Górecka, J. Hobbs, D. Pocięcha, *J. Am. Chem. Soc.* **2025**, 147, 6058–6066.